RNA (2001), *7*:123–132. Cambridge University Press. Printed in the USA.

The stem-loop binding protein forms a highly stable and specific complex with the 3′ stem-loop of histone mRNAs

DANIEL J. BATTLE[1] and JENNIFER A. DOUDNA[1,2]

[1]Department of Molecular Biophysics and Biochemistry, Yale University, New Haven, Connecticut 06520, USA
[2]Howard Hughes Medical Institute, Yale University, New Haven, Connecticut 06520, USA

ABSTRACT

Replication-dependent histone mRNAs end in a highly conserved 26-nt stem-loop structure. The stem-loop binding protein (SLBP), an evolutionarily conserved protein with no known homologs, interacts with the stem-loop in both the nucleus and cytoplasm and mediates nuclear-cytoplasmic transport as well as 3′-end processing of the pre-mRNA by the U7 snRNP. Here, we examined the affinity and specificity of the SLBP–RNA interaction. Nitrocellulose filter-binding experiments showed that the apparent equilibrium dissociation constant (K_d) between purified SLBP and the stem-loop RNA is 1.5 nM. Binding studies with a series of stem-loop variants demonstrated that conserved residues in the stem and loop, as well as the 5′ and 3′ flanking regions, are required for efficient protein recognition. Deletion analysis showed that 3 nt 5′ of the stem and 1 nt 3′ of the stem contribute to the binding energy. These data reveal that the high affinity complex between SLBP and the RNA involves sequence-specific contacts to the loop and the top of the stem, as well the base of the stem and its immediate flanking sequences. Together, these results suggest a novel mode of protein–RNA recognition that forms the core of a ribonucleoprotein complex central to the regulation of histone gene expression.

Keywords: histone mRNA; RNA processing; RNA–protein interactions; stem-loop

INTRODUCTION

Most eukaryotic mRNAs are polyadenylated at their 3′ ends, providing a binding site for several nuclear and cytoplasmic protein factors. These factors control the transport of mRNA from the nucleus, targeting to polyribosomes for translation, and regulation of message stability. The replication-dependent histone mRNAs are the only RNA polymerase II transcripts that lack this poly(A) tail. Instead, the histone pre-mRNAs contain two highly conserved regions at their 3′ terminus: a 26-nt stem-loop structure followed by a purine-rich sequence known as the histone downstream element (HDE; Birnstiel et al., 1985; Marzluff, 1992). These pre-mRNAs are processed in the nucleus by a single endonucleolytic cleavage approximately 5 nt downstream of the stem-loop, catalyzed by the U7 snRNP through base pairing of the U7 snRNA with the HDE (Gick et al., 1986). After processing, the mature messages are exported from the nucleus to the cytoplasm, where they are targeted to polyribosomes and translated (Fig. 1; Eckner et al., 1991; Sun et al., 1992; Williams et al., 1994). These events are tightly coupled to the cell cycle, resulting in high histone mRNA levels immediately preceding DNA replication. This posttranscriptional regulation is responsible for the majority of the cell-cycle dependent control of histone mRNA levels (Schumperli, 1986; Marzluff & Pandey, 1988; Harris et al., 1991).

The stem-loop binding protein (SLBP), a 32-kDa protein with no known homologs, is associated with the stem-loop at the 3′ end of the histone messages in both the nucleus and cytoplasm of higher eukaryotes (Fig. 1; Mowry et al., 1989; Vasserot et al., 1989; Pandey et al., 1991; Hanson et al., 1996; Martin et al., 1997). SLBP levels are cell-cycle regulated, being highest during S-phase when histone mRNA levels are increased (Whitfield et al., 2000). SLBP is necessary for efficient 3′ end processing of histone pre-mRNA by the U7 snRNP (Streit et al., 1993; Dominski et al., 1995). In addition, mutations in the stem-loop that disrupt formation of the SLBP-RNA complex result in the retention of the mRNA in the nucleus and failure to target to polyribosomes (Sun et al., 1992; Williams et al., 1994). These same mutations also disrupt the cell-cycle dependent regulation of histone mRNA stability (Pandey & Marzluff, 1987; Harris et al., 1991). Through these mecha-

Reprint requests to: Jennifer Doudna, Department of Molecular Biophysics and Biochemistry, 266 Whitney Avenue, Bass 334, New Haven, Connecticut 06520, USA; e-mail: doudna@mail.csb.yale.edu.

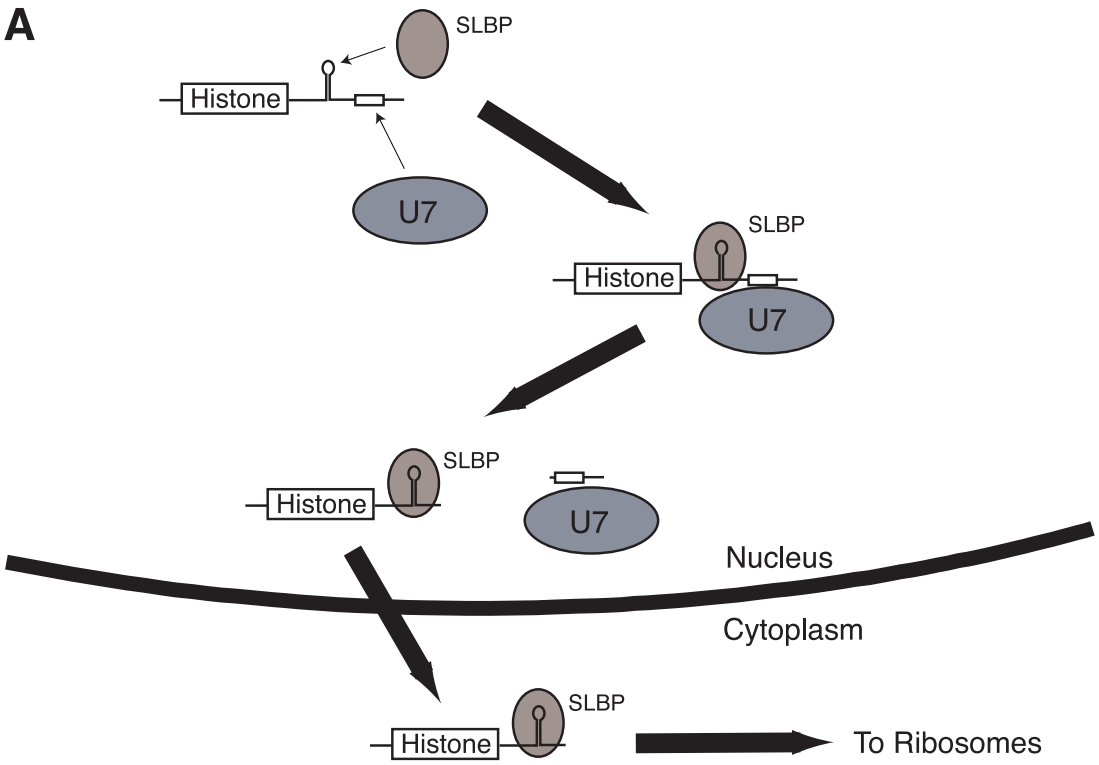

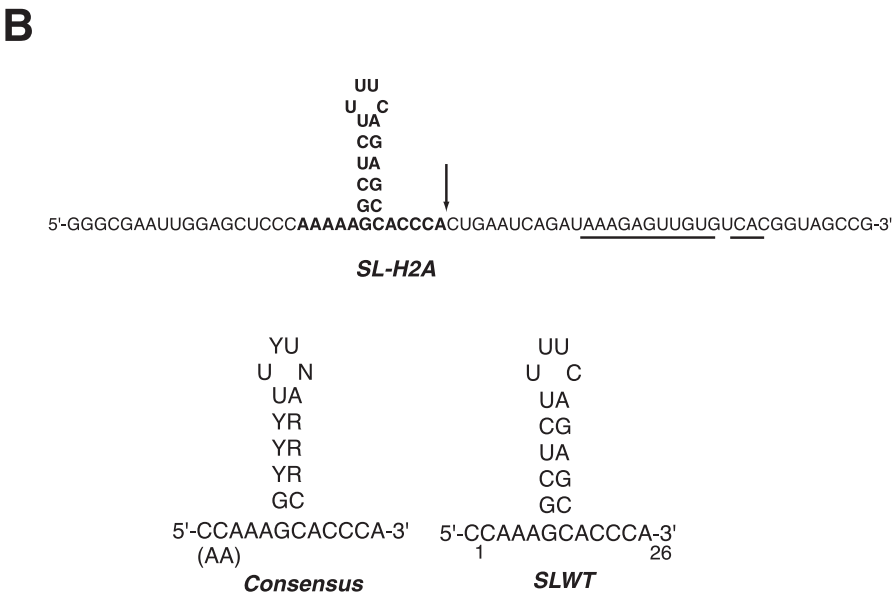

FIGURE 1. SLBP associates with the histone mRNA in the nucleus and cytoplasm. **A**: The role of SLBP in the life cycle of replication-dependent histone mRNAs. The pre-mRNA contains two conserved elements in the 3′ UTR: a 26-nt stem-loop structure and the purine-rich HDE (box) that base-pairs with the U7 snRNA. SLBP is required for efficient 3′ end processing of the pre-mRNA by the U7 snRNP, as well as transport from the nucleus and targeting to polyribosomes. **B**: RNA constructs used to determine the affinity of SLBP for the 3′ UTR of the histone pre-mRNA. SL-H2A is derived from the 3′ UTR of the mouse H2A-614 pre-mRNA. The conserved 26-nt stem-loop structure is in bold and the regions of the HDE proposed to base pair with the mouse U7 snRNA are underlined. SLWT corresponds to the conserved 26-nt stem-loop structure.

nisms, it is believed that formation and maintenance of the SLBP-RNA complex contributes to the cell-cycle regulation of histone levels in higher eukaryotes.

Formation of the SLBP-histone mRNA complex has been previously studied using competition assays in nuclear extract (Williams & Marzluff, 1995). This work

implicated several nucleotides both upstream and downstream of the stem, as well as the conserved sequence of the stem itself, in recognition by SLBP. Other work, however, suggested that SLBP may not directly recognize the flanking region downstream of the stem, adjacent to the 3′ end processing site (Furger et al., 1998). Here we utilize direct in vitro measurements of dissociation constants with purified components to define the affinity and specificity of the SLBP–RNA complex.

RESULTS

SLBP recognizes the 3′ stem-loop of histone mRNAs with high affinity

Nitrocellulose filter-binding experiments were used to examine the energetics of the SLBP–RNA interaction. The affinity of the full-length *Xenopus* SLBP1 for a 78-nt RNA derived from the 3′ UTR of the mouse histone H2A gene was examined (SL-H2A, Fig. 1B). This construct contained the highly conserved 26-nt stem-loop structure as well as the HDE and several nonconserved flanking nucleotides. An apparent equilibrium dissociation constant (K_d) of 0.85 ± 0.3 nM was observed, corresponding to a ΔG of −12.3 ± 0.4 kcal/mol (Table 1). A 26-nt RNA comprising the most conserved elements of the histone mRNA stem-loop (SLWT, Fig. 1B) displayed a similar affinity for both the *Xenopus* and human SLBP (1.5 ± 0.5 nM and 1.2 ± 0.5 nM, respectively) (Table 1, Fig. 2A). This confirms that SLBP primarily recognizes the stem-loop structure within the mRNA. Native gel electrophoresis was used to confirm the presence of a single free and a single bound species in the experiment (data not shown). High concentrations of $MgCl_2$ and KCl disrupted complex formation (Fig. 2B); therefore conditions of 50 mM KCl and 0.5 mM EDTA were used for all subsequent experiments.

Strong specificity determinants are found in the stem, loop, and flanking regions of the RNA

Previous experiments using nuclear extract implicated several residues in the RNA as determinants for SLBP binding specificity (Williams & Marzluff, 1995). Although these experiments link SLBP to the stem-loop RNA, the specificity could have been influenced in part by other components of the nuclear extract. Therefore, we set out to examine the elements in the stem-loop that directly interact with SLBP. We have used direct K_d measurements with purified components to determine the energetic effects of a series of mutations in the conserved stem-loop (Fig. 3). Nitrocellulose filter-binding experiments were used to measure the affinity of SLBP for each of the mutants, and a ΔΔG for each was calculated. Gel-shift experiments resulted in ΔΔG values identical to those measured by filter binding (data not shown).

Mutations in the stem had a dramatic effect on affinity. No binding was observed when all of the base pairs in the stem were replaced by their Watson–Crick complement (SLRS, Fig. 3A), suggesting that if the interaction exists, it was too weak to be observed in the assay (K_d(rel) > 200, ΔΔG > 3.1 kcal/mol; the limit of detection for this assay). To assess the contribution of individual base pairs, the stem-loop was systematically mutated and the binding affinity of each mutant was determined (Fig. 3A). The first and second base pairs at the bottom of the stem are universally conserved G-C pairs. Transversion of the G7-C20 base pair to a C-G (SL-CG2) had a >200-fold effect on the K_d and a ΔΔG of >3.1 kcal/mol, whereas transversion of the G6-C21 pair (SL-CG1) had surprisingly little effect. Transversion of the third base pair in the stem, C8-G19 (SL-GC3), had a moderate 5.6-fold effect on the K_d and a ΔΔG of 1.0 kcal/mol. These data suggest direct, strong contacts to the second and third base pairs of the stem. Transversions of the fourth and fifth base pairs, U9-A18 and C10-G17 (SL-AU4 and SL-GC5), have only small effects on binding affinity. Mutation of the top base pair of the stem from the highly conserved U11-A16 pair to a U-G pair (SL-UG6) resulted in a 15-fold increase of the K_d and a ΔΔG of 1.6 kcal/mol. This effect could be caused by loss of a direct protein contact, and/or by a change in the secondary structure at the top of the stem resulting in a change in the structure of the loop. Together, these data suggest that there are 3 bp within the stem that are critical for protein recognition.

Next, we investigated the effect of mutations in the loop region on SLBP binding (Fig. 3C,D). Previous work had implicated U12 and U14 as playing a role in SLBP recognition (Williams & Marzluff, 1995). This was confirmed, as mutation of both of those uracils to A (SL-AUAC) resulted in no detectable binding to SLBP. Possible explanations for this effect include direct contact between SLBP and one or both of the two U residues in the loop, or destabilization of the loop and top of the stem by the AUAC loop. Alternatively, U12 and C15 could be involved in a U-C base pair critical for maintaining a correct backbone structure for SLBP recognition. To investigate these possibilities, we created

TABLE 1. Results of nitrocellulose filter-binding experiments with the full-length *Xenopus* SLBP1 and the human SLBP proteins. The K_d and ΔG values reported here are the average values from at least three independent experiments. Errors are standard deviations.

Protein/RNA construct	K_d (nM)	ΔG (kcal/mol)
xSLBP1/SL-H2A	0.85 ± 0.3	−12.3 ± 0.4
xSLBP1/SLWT	1.5 ± 0.5	−12.0 ± 0.3
hSLBP/SLWT	1.2 ± 0.5	−12.2 ± 0.2

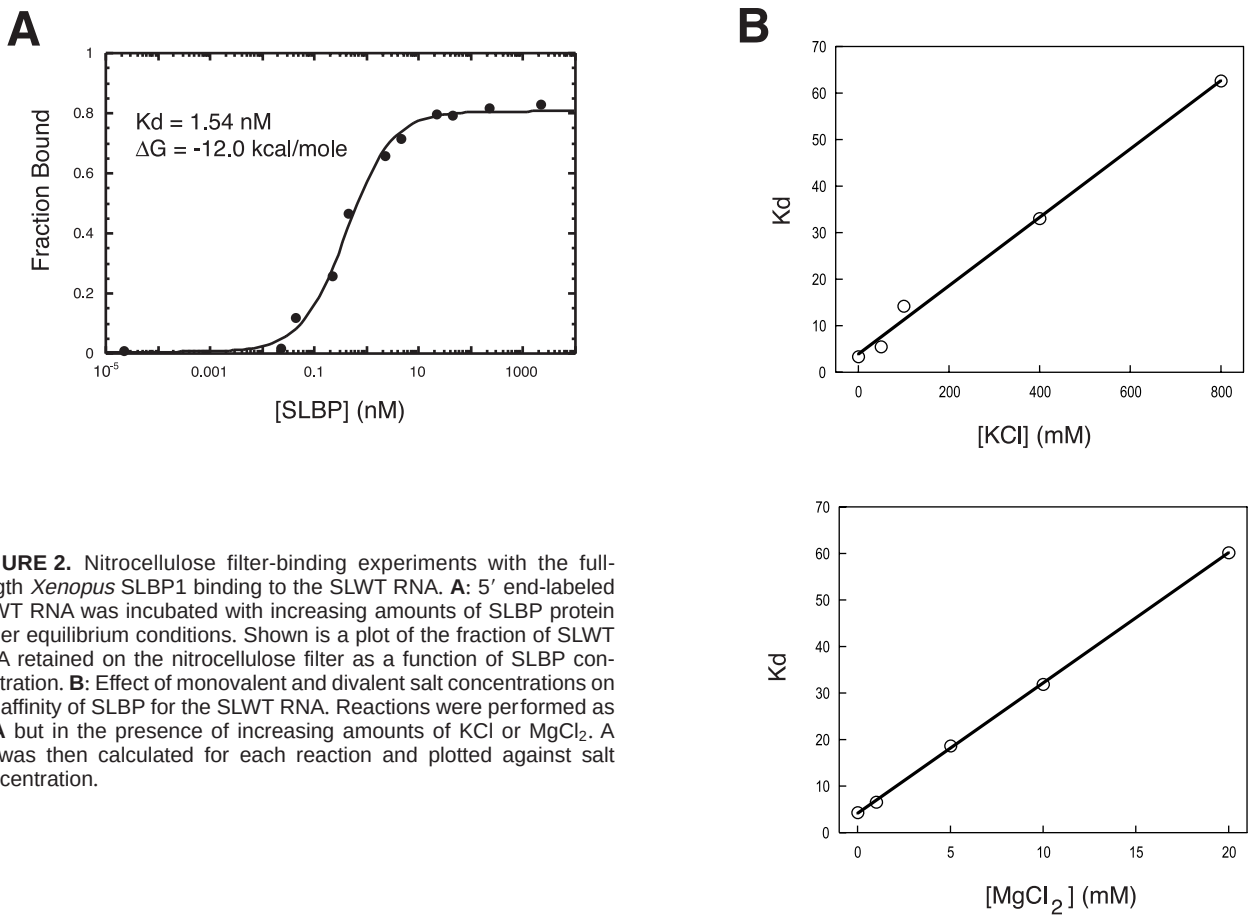

FIGURE 2. Nitrocellulose filter-binding experiments with the full-length *Xenopus* SLBP1 binding to the SLWT RNA. **A**: 5′ end-labeled SLWT RNA was incubated with increasing amounts of SLBP protein under equilibrium conditions. Shown is a plot of the fraction of SLWT RNA retained on the nitrocellulose filter as a function of SLBP concentration. **B**: Effect of monovalent and divalent salt concentrations on the affinity of SLBP for the SLWT RNA. Reactions were performed as in **A** but in the presence of increasing amounts of KCl or $MgCl_2$. A K_d was then calculated for each reaction and plotted against salt concentration.

two other loop mutants: L-GUUA and L-GNRA (Fig. 3C). L-GNRA is a well-characterized stable tetraloop. If the loss of binding of L-AUAC were simply due to loop instability leading to the failure to form the proper 6-bp stem, binding should be restored in the L-GNRA mutant. L-GUUA allows for the possibility of a GNRA style base pair at the 12–15 position, but retains the conserved U at position 14. All of the loop mutants showed similar UV melting profiles to SLWT and showed similar mobilities by native gel electrophoresis (data not shown). No binding was detected with either the L-GNRA or the L-GUUA mutant. We then mutated positions U12 and U14 individually. Mutation of either U12 or U14 to adenosine (L-AUUC, L-UUAC) had dramatic effects on binding, although neither was as deleterious as mutation of both positions together. If the effect of mutation of either U12 or U14 is the result of interfering with the overall loop backbone geometry, mutation of a single position should show the same effect as the double mutant. Instead, these results suggest that SLBP directly recognizes both U12 and U14 in a base-specific manner, rather than requiring only the stability of the loop or overall loop geometry.

We also examined whether SLBP makes direct contact to bases in both the 5′ and 3′ flanking regions (Fig. 4). Deletion of both entire 5′ and 3′ flanking regions abolished binding in our assay. Mutation of the first three residues 3′ of the stem from ACC to GGG had previously been shown to affect binding in nuclear extract, but mutation of the first two residues from AC to GA still allowed SLBP binding in extract, and the resulting complex was capable of 3′ end processing (Williams & Marzluff, 1995; Furger et al., 1998). We found that binding to the SL-3′GGGCA mutant was reduced (K_d(rel) = 6.4, $\Delta\Delta G$ = 1.1 kcal/mol). This effect could be due to direct contacts within this region or to changes in the secondary structure, as the three guanosine residues could form base pairs with the nucleotides 5′ of the stem. To differentiate between these two possibilities, we performed a systematic deletion analysis (Fig. 4). We found that deletion of 4 nt from the 3′ end had virtually no effect on binding, whereas deletion of the entire 3′ flanking region had a 5.5-fold effect, suggesting that position A22 is critical for protein recognition. We performed a similar deletion analysis from the 5′ end. Deletion of the first two C residues had no effect on binding. Deletion of position A3, however, had a moderate effect (SL-5′Δ3, K_d(rel) = 5.4), and deletion of four residues had a large 13.7-fold effect on K_d. From this, we conclude that there is likely a contact to position A3 and a critical contact to A4.

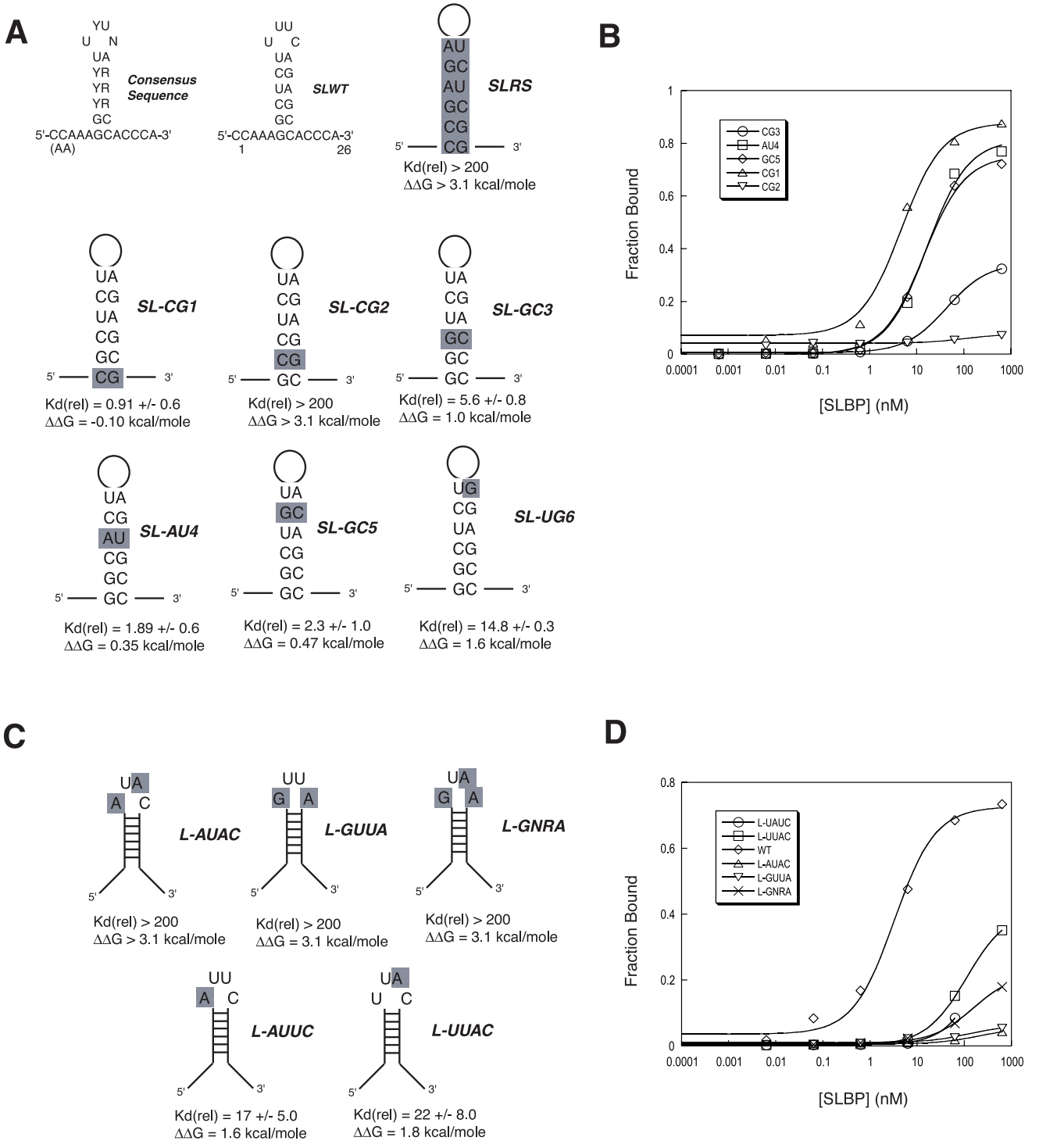

FIGURE 3. Effect of mutations in the stem and loop regions of the RNA on SLBP affinity. **A**: Equilibrium nitrocellulose filter-binding experiments were performed with several RNAs mutated in the 6-bp stem region. All mutants retain the SLWT sequence in the loop and 5′ and 3′ flanking regions. Mutant SLRS has all 6 bp in the stem replaced by their Watson–Crick complement. SL-CG1 through SL-GC5 contain transversions of the each of the first 5 bp of the stem. SL-UG6 has the top base pair of the stem mutated to a U-G pair. The SLWT and consensus sequences are shown for comparison. For each mutant, a K_d(rel) and ΔΔG were calculated where K_d(rel) = K_d(mutant)/K_d(SLWT), and the ΔΔG is taken relative to the ΔG of the SLWT-xSLBP1 interaction. **B**: Representative binding curves for some of the stem mutants. **C**: Similar reactions were performed with RNAs containing mutations in the loop region. All mutants retain the SLWT sequence in the stem and flanking regions and have the sequence shown for the loop region. **D**: Representative binding curves for some of the loop mutants.

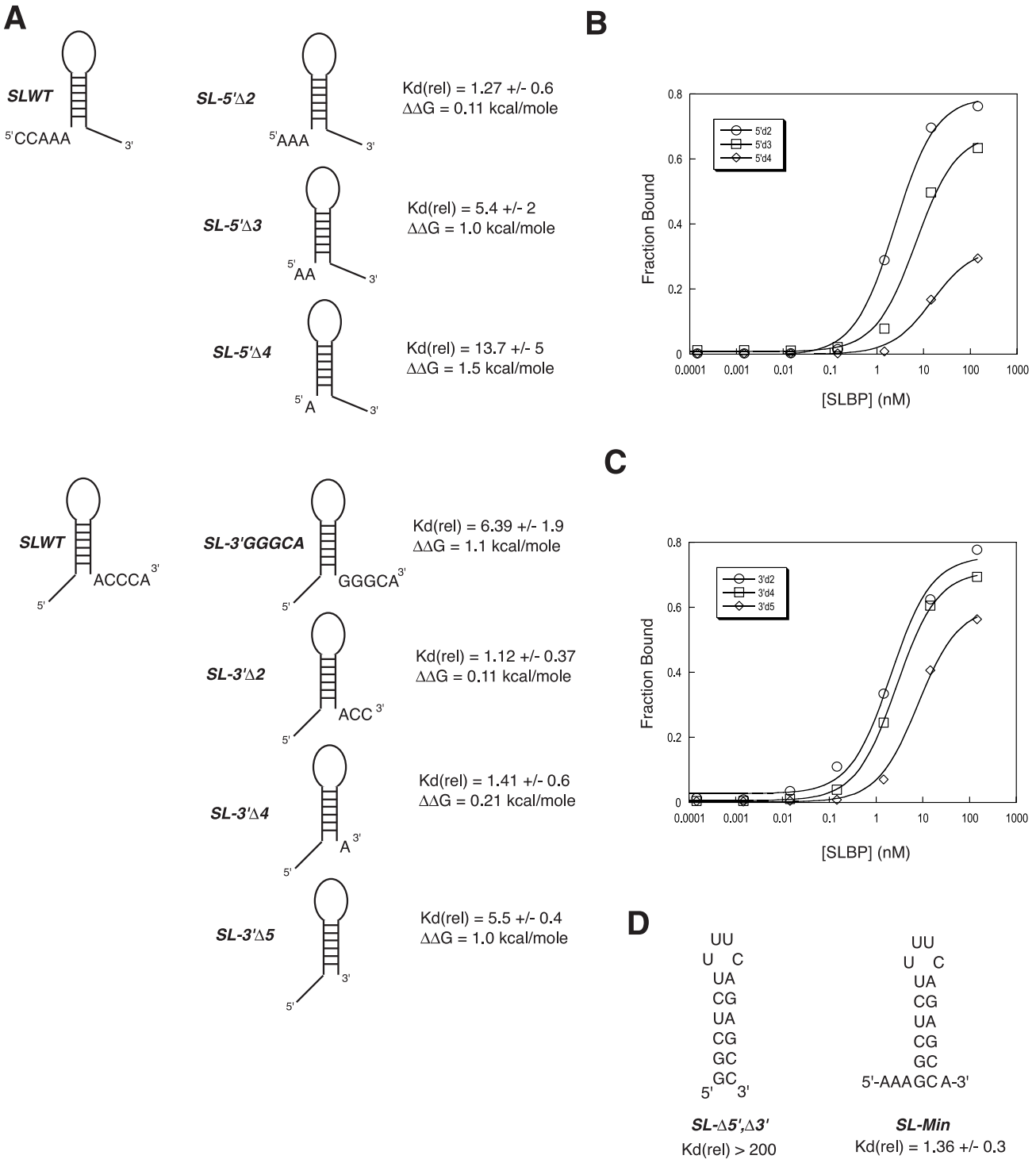

FIGURE 4. Deletion analysis of the SLBP-RNA complex. **A** and **D**: Nitrocellulose filter-binding experiments were performed under equilibrium conditions with several RNAs with deletions from their 5′ or 3′ ends. All RNAs retain the SLWT sequence except where otherwise specified. SL-3′GGGCA has the first three bases 3′ of the stem mutated to G. SL-Δ5′,Δ3′ has the entire 5′ and 3′ flanking regions removed. SL-Min is the 20-nt minimal RNA capable of being recognized by SLBP with high affinity. For each mutant, a K_d(rel) and ΔΔG were calculated where K_d(rel) = K_d(mutant)/K_d(SLWT), and the ΔΔG is taken relative to the ΔG of the SLWT-xSLBP1 interaction. **B** and **C**: Representative binding curves for each of the 5′ and 3′ deletion mutants.

These data suggest that the minimal RNA capable of recognition with high affinity by SLBP is a 20-nt RNA consisting of the conserved stem-loop motif flanked by three conserved adenosines on the 5′ end, and one conserved adenosine on the 3′ end. To test this, we created mutant SL-Min (Fig. 4D). As expected, this con-

struct bound SLBP with near wild-type affinity (K_d(rel) = 1.36 ± 0.3).

DISCUSSION

Replication-dependent histone mRNAs contain a 26-nt stem-loop structure at their 3′ terminus. The sequence of the stem-loop, as well as the sequence immediately flanking the stem-loop, is highly conserved among all metazoans. SLBP is found associated with this stem-loop in both the nucleus and cytoplasm of higher eukaryotes (Mowry et al., 1989; Vasserot et al., 1989; Pandey et al., 1991; Hanson et al., 1996; Martin et al., 1997). Mutations that disrupt formation of the SLBP-RNA complex in nuclear extract interfere with proper pre-mRNA processing, as well as mature mRNA localization and cell-cycle dependent stability (Pandey & Marzluff, 1987; Harris et al., 1991; Sun et al., 1992; Streit et al., 1993; Williams et al., 1994; Dominski et al., 1995). Here we have used direct K_d measurements with purified protein and RNA components to define the affinity and specificity of the SLBP-histone mRNA interaction.

Nitrocellulose filter-binding experiments were performed to determine the affinity of SLBP for the RNA stem-loop. This interaction was found to be quite tight, with a K_d = 1.5 nM, corresponding to a ΔG of −12.0 kcal/mol. The measured affinity was strongly affected by ionic strength, dropping off quickly with increasing concentrations of $MgCl_2$ or KCl (Fig. 2). This suggests that electrostatics play a key role in recognition of the stem-loop by SLBP, similar to what is commonly observed for many complexes involving protein recognition of a simple DNA duplex (Misra et al., 1994). However, even at very high salt concentration (800 mM KCl), binding was still relatively tight (60 nM), suggesting that hydrophobics contribute to the interaction, perhaps through recognition of the loop or flanking nucleotides.

As observed previously in extracts, mutations in the 6-bp stem greatly reduced SLBP binding (Fig. 3A). The bottom 2 bp are invariantly G-C base pairs. Previous work had shown a large drop in binding affinity upon transversion of the bottom two G-C base pairs together (Williams & Marzluff, 1995). We found that transversion of the bottom base pair alone had no detectable effect on binding, whereas transversion of the second base pair (G7-C20) led to a marked increase in the K_d. In addition, we found that mutation of the third base pair, always a pyrimidine-purine pair, to G-C also had a strong, negative effect on binding. Similarly, mutation of the invariant U-A pair at the top of the stem had a dramatic deleterious effect on SLBP binding. Taken together, these data suggest multiple SLBP contacts to the RNA stem, particularly to base pairs G7-C20, C8-G19, and U11-A16 (Fig. 5). Some of these effects could result from subtle changes in the helical parameters that reposition specificity determinants in the loop relative to the base of the stem or flanking regions.

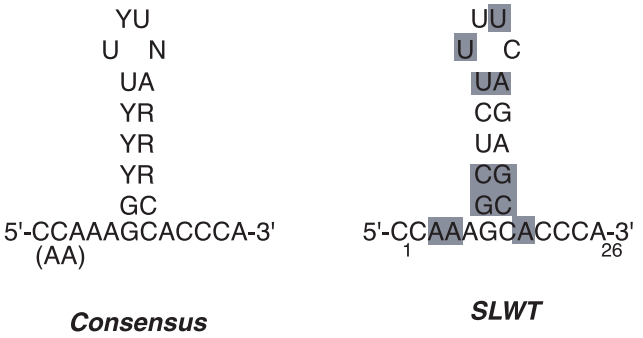

FIGURE 5. A comparison of the consensus sequence of the histone mRNA 3′ stem-loop with the specificity determinants for SLBP recognition. Shown in gray boxes are nucleotides that show a deleterious effect on SLBP affinity when mutated or deleted.

The first and third positions of the loop are also highly evolutionarily conserved. The first position is a U except in *Caenorhabditis elegans*, where it is a C, and the third position is invariantly a U. Mutation of the loop from UUUC to AUAC, GUUA, or GUAA abolished binding, and single mutations of positions U12 and U14 both had dramatic effects on binding (Fig. 3C). This suggests critical, sequence-specific contacts between SLBP and the first and third positions of the loop.

The 5 nt immediately 5′ of the stem are highly conserved, with a consensus of C or A at positions 1 and 2, and adenosines at positions 3, 4, and 5. We have found that the first two positions can be deleted with no effect on SLBP binding (Fig. 4). They may be conserved as C or A simply to prevent them from forming deleterious base pairs with the conserved C and A residues 3′ of the stem. However, deletion of position 3 had a moderate effect and deletion of position 4 had a strong effect on SLBP recognition. This suggests that SLBP makes critical contacts at positions 3 and 4. Alternatively, adenosine residues in general, and multiple adenosine residues in particular, are often found to make tertiary RNA–RNA contacts (Pley et al., 1994; Cate et al., 1996; Costa & Michel, 1997; Strobel et al., 1998), leading to the possibility of a strained base-triple or pseudoknot structure involving A3 or A4. However, divalent cations are often required for these interactions, whereas here the specificity of the interaction was maintained in the absence of Mg^{2+} and the presence of EDTA, and SLBP binding in fact was reduced by the presence of $MgCl_2$. This makes the possibility of a more complex structure unlikely.

Similarly, the ACCCA sequence 3′ of the stem is also highly conserved. The major position of cleavage by the U7 snRNP is immediately 3′ of A26, and efficiency of this cleavage is dependent on SLBP (Streit et al., 1993; Dominski et al., 1995). These considerations suggested that SLBP may contact the 3′ flanking region

and orient it for cleavage by the U7 snRNP. We found, however, that much of the 3′ flanking region could be deleted without a large effect on the affinity of the SLBP-RNA interaction (Fig. 4). Deletion of four of the residues had only a slight effect, and deletion of the entire 3′ flanking region increased the K_d 5.5-fold. This suggests that SLBP is not making extensive contacts to most of this region, but rather is only interacting with the first A residue 3′ of the stem. Alternatively, the presence of a 3′ overhanging adenosine has been shown to contribute approximately 1 kcal/mol to the stability of short oligonucleotide duplexes (Freier et al., 1986). It is possible, therefore, that A22 simply serves to stabilize the stem and is not contacting SLBP. These data suggest that SLBP may enhance 3′-end processing by direct or indirect recruitment of the U7 snRNP to the cleavage site as has been previously proposed (Dominski et al., 1999), rather than by directly ordering the RNA structure at the cleavage site. The sequence conservation of the 3′ flanking region (and possibly the bottom G-C pair of the stem) may be necessary for the binding of other components of the 3′-end processing machinery.

SLBP has no homology with any other proteins thus far discovered. It contains a relatively small, approximately 73 amino acid, RNA-binding domain predicted to contain three α-helices (Wang et al., 1996; Martin et al., 2000). Previously characterized RNA-binding domains (Draper, 1999) recognize either the loop in a sequence-specific manner, as with U1A (Oubridge et al., 1994), or the loop and end of a stem by relying on noncanonical base pairs or bulges to insert helices into the major groove, as in the bacteriophage lambda N peptide (Legault et al., 1998). Others recognize Watson–Crick A-form RNA helices in a predominantly sequence-independent manner (Ryter & Schultz, 1998). SLBP, on the other hand, makes sequence-specific contacts with the loop and top of a Watson–Crick stem, as well as the base of the stem and several flanking nucleotides (Fig. 5). As such, SLBP likely represents a novel mode of protein–RNA recognition.

MATERIALS AND METHODS

Preparation of SLBP

Recombinant baculoviruses for the human SLBP as well as the *Xenopus* SLBP1 were obtained from Bill Marzluff at the University of North Carolina. SF9 insect cells were grown in suspension culture to a density of 10^6 cells/mL in Grace's insect medium supplemented with 10% fetal bovine serum. The cells were infected with recombinant baculoviruses at a multiplicity of infection (MOI) = 10, and the infection was allowed to proceed for 5 days. Cells were pelleted and lysed in a buffer containing 25 mM Tris-HCl, pH 8.0, 300 mM KCl, 0.01% Nonidet P-40, and 0.1 mM PMSF. The clarified lysate was bound on a column packed with Ni-NTA resin and eluted in 25 mM Tris-HCl, pH 8.0, 300 mM KCl, and 300 mM imidazole. The protein was then dialyzed overnight into 25 mM HEPES, pH 7.5, 50 mM KCl, 1 mM DTT, and 0.5 mM EDTA and then passed over a Mono-S column. After elution with a gradient of KCl, the protein was dialyzed into a storage buffer with 25 mM Tris-HCl, pH 7.5, 50 mM KCl, 1 mM DTT, 0.5 mM EDTA, and 20% glycerol and stored at −80 °C.

Preparation of RNA constructs

pUC19 plasmids were constructed containing the SLWT sequence flanked on the 5′ end by a T7 RNA polymerase promoter and a hairpin ribozyme, and on the 3′ end by the recognition sequence for the VS ribozyme. After linearization with the *Bsa*I restriction enzyme, run-off transcription with T7 RNA polymerase in the presence of VS ribozyme yielded the 26-nt RNA constructs (Ferre-D'Amare & Doudna, 1996). pUC19 plasmids containing the SL-H2A, SLWT, GGG, UG, and RS sequences were constructed and linearized with *Bsa*I. Run-off transcription with T7 RNA polymerase yielded the 78- or 26-nt constructs preceded by two extra guanosine residues. All remaining RNA constructs as well as additional SLWT RNA were synthesized by Dharmacon Research Inc. (Boulder, Colorado). The RNAs were then deprotected as per manufacturer's specifications and 5′ labeled directly. There were no differences in activity between SLWT RNAs prepared by any of the three methods.

Nitrocellulose filter-binding experiments

Binding constants were determined by a nitrocellulose filter-binding experiment (Pata et al., 1995). 5′ end-labeled RNA at a concentration <50 pM was incubated with increasing amounts of protein in 50 μL of 1× binding buffer (25 mM Tris-HCl, pH 7.5, 50 mM KCl, 0.5 mM EDTA, 1 mM DTT, 0.01% Nonidet P-40, 1 μg/μL tRNA) for 1 h at 25 °C. Binding was found to be independent of tRNA concentration, but strongly dependent on salt concentration. The mixture was passed first over a 0.45 μm filter, then a nitrocellulose filter, and finally a Hybond-N+ positively charged filter. The filters were then washed with 100 μL of wash buffer (25 mM Tris-HCl, pH 7.5, 100 mM KCl) and then allowed to air dry for 30 min. Retention of the SLBP-SLWT complex on the nitrocellulose was independent of washing the filter with buffer. In fact, it was found that the filter could be soaked in aqueous buffer for several hours without releasing SLWT, suggesting a very slow off rate for the complex.

The filters were imaged using a Molecular Dynamics phosphorimager and the program ImageQuaNT. The resulting data were analyzed using Microsoft Excel and Kaleidagraph. Background intensities (<10% of the total intensity of each spot) were subtracted from the intensities of all spots. The fraction bound was then calculated to be the intensity of the spot on the nitrocellulose filter divided by the sum of the spots on the nitrocellulose and Hybond-N+ filters. A least squares fit for a single binding site was obtained using the equation

$$f = (a - b)[P/(P + K_d)] + b,$$

where a is the maximum fraction bound at saturating SLBP, b is the amount theoretically bound in the absence of SLBP, P is the active SLBP concentration, and K_d is the apparent equilibrium dissociation constant. All K_d and $\Delta\Delta G$ values re-

ported are the average values from at least three independent experiments.

SLBP activity assay

Each preparation of SLBP was assayed for activity using a stoichiometry assay. Nitrocellulose filter-binding experiments were carried out as described above, except that the 5′-end-labeled SLWT RNA was supplemented with cold SLWT RNA to a final concentration in the reaction of 640 nM. The data were fit to the equation

$$f = (a - b)[[K_d + P + R_t - ((K_d + P + R_t)^2 - 4R_tP)^{1/2}]/2R_t] + b,$$

where a is the maximum fraction bound at saturating SLBP, b is the amount theoretically bound in the absence of SLBP, K_d is the apparent dissociation constant, P is protein concentration, and R_t is the concentration of SLBP giving a 1:1 complex with the SLWT. Protein activity was adjusted to fit the 1:1 stoichiometry.

ACKNOWLEDGMENTS

We would like to thank Joshua Davis and Rowena McBeath for technical assistance, William Marzluff and lab for recombinant baculoviruses, Robert Batey, Elizabeth Doherty, Peter Adams, and Jeff Kieft for comments on the manuscript, and all members of the Doudna lab for helpful discussions.

Received September 6, 2000; returned for revision October 17, 2000; revised manuscript received October 20, 2000

REFERENCES

Birnstiel ML, Busslinger M, Strub K. 1985. Transcription termination and 3′ processing: The end is in site! *Cell 41*:349–359.

Cate JH, Gooding AR, Podell E, Zhou K, Golden BL, Kundrot CE, Cech TR, Doudna JA. 1996. Crystal structure of a group I ribozyme domain: Principles of RNA packing [see comments]. *Science 273*:1678–1685.

Costa M, Michel F. 1997. Rules for RNA recognition of GNRA tetraloops deduced by in vitro selection: Comparison with in vivo evolution. *EMBO J 16*:3289–3302.

Dominski Z, Sumerel J, Hanson RJ, Whitfield ML, Marzluff WF. 1995. The polyribosomal protein bound to the 3′ end of histone mRNA can function in histone pre-mRNA processing. *Nucleic Acids Symp Ser 33*:234–236.

Dominski Z, Zheng LX, Sanchez R, Marzluff WF. 1999. Stem-loop binding protein facilitates 3′-end formation by stabilizing U7 snRNP binding to histone pre-mRNA. *Mol Cell Biol 19*:3561–3570.

Draper DE. 1999. Themes in RNA–protein recognition. *J Mol Biol 293*:255–270.

Eckner R, Ellmeier W, Birnstiel ML. 1991. Mature mRNA 3′ end formation stimulates RNA export from the nucleus. *EMBO J 10*:3513–3522.

Ferre-D'Amare AR, Doudna JA. 1996. Use of *cis*- and *trans*-ribozymes to remove 5′ and 3′ heterogeneities from milligrams of in vitro transcribed RNA. *Nucleic Acids Res 24*:977–978.

Freier SM, Kierzek R, Jaeger JA, Sugimoto N, Caruthers MH, Neilson T, Turner DH. 1986. Improved free-energy parameters for predictions of RNA duplex stability. *Proc Natl Acad Sci USA 83*:9373-9377.

Furger A, Schaller A, Schumperli D. 1998. Functional importance of conserved nucleotides at the histone RNA 3′ processing site. *RNA 4*:246–256.

Gick O, Kramer A, Keller W, Birnstiel ML. 1986. Generation of histone mRNA 3′ ends by endonucleolytic cleavage of the pre-mRNA in a snRNP-dependent in vitro reaction. *EMBO J 5*:1319–1326.

Hanson RJ, Sun J, Willis DG, Marzluff WF. 1996. Efficient extraction and partial purification of the polyribosome-associated stem-loop binding protein bound to the 3′ end of histone mRNA. *Biochemistry 35*:2146–2156.

Harris ME, Bohni R, Schneiderman MH, Ramamurthy L, Schumperli D, Marzluff, WF. 1991. Regulation of histone mRNA in the unperturbed cell cycle: Evidence suggesting control at two posttranscriptional steps. *Mol Cell Biol 11*:2416–2424.

Legault P, Li J, Mogridge J, Kay LE, Greenblatt, J. 1998. NMR structure of the bacteriophage lambda N peptide/boxB RNA complex: Recognition of a GNRA fold by an arginine-rich motif. *Cell 93*: 289–299.

Martin F, Michel F, Zenklusen D, Muller B, Schumperli D. 2000. Positive and negative mutant selection in the human hairpin-binding protein using the yeast three-hybrid system. *Nucleic Acids Res 28*:1594–1603.

Martin F, Schaller A, Eglite S, Schumperli D, Muller B. 1997. The gene for histone RNA hairpin binding protein is located on human chromosome 4 and encodes a novel type of RNA binding protein. *EMBO J 16*:769–778.

Marzluff WF. 1992. Histone 3′ ends: Essential and regulatory functions. *Gene Expr 2*:93–97.

Marzluff WF, Pandey NB. 1988. Multiple regulatory steps control histone mRNA concentrations. *Trends Biochem Sci 13*:49–52.

Misra VK, Hecht JL, Sharp KA, Friedman RA, Honig B. 1994. Salt effects on protein–DNA interactions. The lambda cI repressor and *Eco*RI endonuclease. *J Mol Biol 238*:264–280.

Mowry KL, Oh R, Steitz JA. 1989. Each of the conserved sequence elements flanking the cleavage site of mammalian histone pre-mRNAs has a distinct role in the 3′-end processing reaction. *Mol Cell Biol 9*:3105–3108.

Oubridge C, Ito N, Evans PR, Teo CH, Nagai K. 1994. Crystal structure at 1.92 Å resolution of the RNA-binding domain of the U1A spliceosomal protein complexed with an RNA hairpin. *Nature 372*:432–438.

Pandey NB, Marzluff WF. 1987. The stem-loop structure at the 3′ end of histone mRNA is necessary and sufficient for regulation of histone mRNA stability. *Mol Cell Biol 7*:4557–4559.

Pandey NB, Sun JH, Marzluff, WF. 1991. Different complexes are formed on the 3′ end of histone mRNA with nuclear and polyribosomal proteins. *Nucleic Acids Res 19*:5653–5659.

Pata JD, Schultz SC, Kirkegaard K. 1995. Functional oligomerization of poliovirus RNA-dependent RNA polymerase. *RNA 1*:466–477.

Pley HW, Flaherty KM, McKay DB. 1994. Three-dimensional structure of a hammerhead ribozyme [see comments]. *Nature 372*: 68–74.

Ryter JM, Schultz SC. 1998. Molecular basis of double-stranded RNA–protein interactions: Structure of a dsRNA-binding domain complexed with dsRNA. *EMBO J 17*:7505–7513.

Schumperli D. 1986. Cell-cycle regulation of histone gene expression. *Cell 45*:471–472.

Streit A, Koning TW, Soldati D, Melin L, Schumperli D. 1993. Variable effects of the conserved RNA hairpin element upon 3′ end processing of histone pre-mRNA in vitro. *Nucleic Acids Res 21*:1569–1575.

Strobel SA, Ortoleva-Donnelly L, Ryder SP, Cate JH, Moncoeur E. 1998. Complementary sets of noncanonical base pairs mediate RNA helix packing in the group I intron active site. *Nat Struct Biol 5*:60–66.

Sun J, Pilch DR, Marzluff WF. 1992. The histone mRNA 3′ end is required for localization of histone mRNA to polyribosomes. *Nucleic Acids Res 20*:6057–6066.

Vasserot AP, Schaufele FJ, Birnstiel ML. 1989. Conserved terminal hairpin sequences of histone mRNA precursors are not involved in duplex formation with the U7 RNA but act as a target site for a distinct processing factor. *Proc Natl Acad Sci USA 86*:4345–4349.

Wang ZF, Whitfield ML, Ingledue TC 3rd, Dominski Z, Marzluff WF. 1996. The protein that binds the 3′ end of histone mRNA: A novel

RNA-binding protein required for histone pre-mRNA processing. *Genes & Dev 10*:3028–3040.

Whitfield ML, Zheng LX, Baldwin A, Ohta T, Hurt MM, Marzluff WF. 2000. Stem-loop binding protein, the protein that binds the 3′ end of histone mRNA, is cell cycle regulated by both translational and posttranslational mechanisms. *Mol Cell Biol 20*:4188–4198.

Williams AS, Ingledue TC 3rd, Kay BK, Marzluff WF. 1994. Changes in the stem-loop at the 3′ terminus of histone mRNA affects its nucleocytoplasmic transport and cytoplasmic regulation. *Nucleic Acids Res 22*:4660–4666.

Williams AS, Marzluff WF. 1995. The sequence of the stem and flanking sequences at the 3′ end of histone mRNA are critical determinants for the binding of the stem-loop binding protein. *Nucleic Acids Res 23*:654–662.